ELSEVIER

Materials Science and Engineering A282 (2000) 164–169

MATERIALS SCIENCE & ENGINEERING A

www.elsevier.com/locate/msea

Properties of titanium nitride fabricated on stainless steel by plasma-based ion implantation/deposition

X.B. Tian, Z.M. Zeng, B.Y. Tang, K.Y. Fu, D.T.K. Kwok, P.K. Chu *

Department of Physics and Materials Science, City University of Hong Kong, 83, Tat Chee Avenue, Kowloon, Hong Kong

Received 11 May 1999; received in revised form 5 November 1999

Abstract

Plasma-based ion implantation (PBII) is a burgeoning surface treatment technique as it offers the possibility of treating complex-shaped and large samples without target manipulation. However, the technique has not been widely adopted in the metallurgical industry due to the difficulty to achieve a thick modified layer at low temperature. In this paper, we describe a method combining PBII and ion mixing to synthesize titanium nitride (TiN) on 304 stainless steel. Titanium and nitrogen ions are generated by a metal arc plasma source and hot filament glow discharge, respectively. By using three different sets of experimental conditions, we investigate the effects of different implantation and deposition parameters on the surface properties of TiN. Results from Auger electron spectroscopy, glancing X-ray diffraction, pin-on-disk test, and microhardness determination reveal significantly improved tribological properties. The enhancement is a consequence of the synergistic effects of the coexistence of titanium, oxygen, and nitrogen, as well as the ion mixed interface.

Keywords: Stainless steel; Titanium nitride; Tribological properties; Plasma-based ion implantation

1. Introduction

Plasma-based ion implantation (PBII) is a fledgling technique to enhance the surface properties of materials and industrial components [1–4]. The non line-of-sight advantage obviates the need for complicated sample manipulation and beam scanning techniques when treating complex-shaped samples. However, owing to the limited energy range in ion implantation, electronic and nuclear stopping in the substrate leads to rapid deceleration of the implanted species, and it is difficult to fabricate a modified layer thick enough for practical or industrial use. It has been shown that elevated temperature ion implantation (both beam-line and plasma-based) can yield thicker layers by combining energetic ion introduction with thermal and transient-enhanced diffusion [5–7]. The thicker layer can endure more wear and tear and better cope with the harsh environment in real engineering applications or in the field. Unfortunately, elevated temperature ion implantation processes such as ion nitriding or carburizing are not universally applicable due to thermal conflicts, strict dimension tolerance, or low melting point of the treated materials. For instance, ion implantation into aluminum alloys at over 300°C can lead to material softening and other deleterious effects [8]. Hence, there is the need to design a low temperature process to take advantage of the non line-of-sight and high throughput benefits of plasma-based ion implantation. A technique employing dynamic mixing in concert with plasma-based ion implantation/deposition offers several advantages: (1) efficient treatment of non-planar targets without sample manipulation, (2) low temperature, (3) good adhesion between the film and substrate, and (4) versatile process with parameters such as deposition rate, implantation rate, ion energy, plasma density, plasma gas pressure, and so on individually adjustable. Conrad et al. [9] used helium and nitrogen plasma immersion ion implantation (PIII) to process TiN and Ti films, respectively. Matossian [10] treated TiN coatings on high-speed steel cutting tools with nitrogen PIII. In addition, formation of nitride or oxide of titanium, niobium, aluminum, and copper has been demonstrated by reactive ion implantation/absorption

* Corresponding author. Tel.: +852-27887724; fax: +852-27889549.

E-mail address: paul.chu@cityu.edu.hk (P.K. Chu)

0921-5093/00/$ - see front matter
PII: S0921-5093(99)00756-X

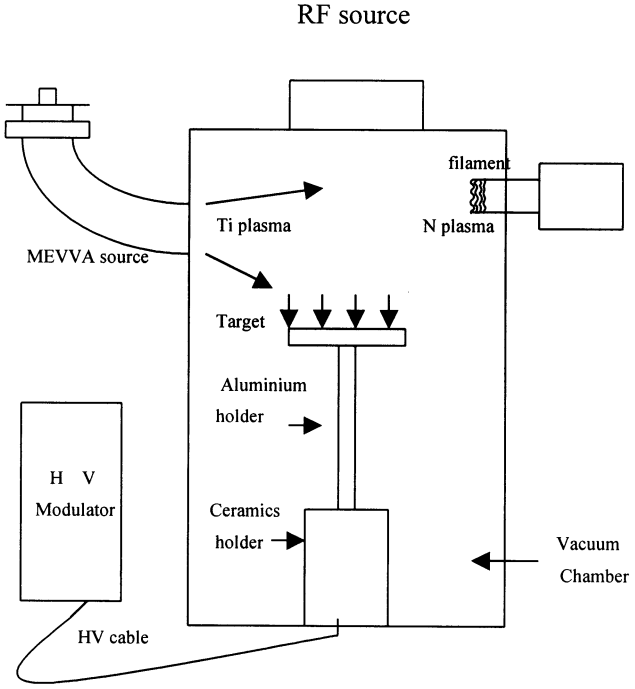

Fig. 1. Schematic of the plasma immersion ion implantation equipment. Four sets of electron emitting filaments and four sets of MEVVA sources are positioned symmetrically around the vacuum chamber.

[11–14]. Recently, the combination of PIII and unbalanced magnetron sputtering from TiN has been reported [15]. In this paper, we present a different method utilizing metal vacuum arc and hot filament glow discharge to obtain titanium and nitrogen plasma for implantation and deposition. Titanium is deposited onto the stainless steel during the 'off-cycle' of the sample high voltage pulses and implanted at the sample bias during the 'on-cycle'. The incorporation of nitrogen via implantation enhances the properties of the TiN films.

2. Experimental

A schematic of the plasma immersion ion implanter used in this work is displayed in Fig. 1 and has been described in details elsewhere [16]. The nitrogen plasma was sustained by hot filament glow discharge in the main vacuum chamber, and the titanium plasma was generated in the metal vacuum arc plasma source (MEVVA) and diffused into the vacuum chamber. The plasma in the vacuum chamber thus contained titanium, nitrogen, or both titanium and nitrogen ions. To reduce sample heating, a medium plasma density of 6.0×10^8 cm^{-3} for nitrogen and 1.0×10^{11} cm^{-3} for titanium was selected. The plasma density was measured by a Langmuir probe prior to each experiment. A 25 mm diameter SS304 stainless steel bar was cut into 4 mm thick discs. One side of each sample was polished to a mirror finish using standard metallographic techniques. The SS304 stainless steel samples were laid on the sample platen connected to a high voltage power modulator. During the negative high voltage pulses, pure titanium ions, pure nitrogen ions, or both of them were implanted into the exposed surface at the applied voltage since the pressure inside the vacuum chamber was low enough that collisionless conditions were met. During the 'off-cycles' of the power modulator, titanium condensed while nitrogen and oxygen were absorbed onto the sample surface. We conducted three experiments using different conditions and the instrumental parameters and processes are listed in Tables 1 and 2.

3. Results and discussion

The samples were depth profiled using Auger electron spectroscopy (AES) to determine the elemental composition and film thickness. The film thicknesses of the samples treated by the three processes described in Table 1 are shown in Fig. 2, whereas the AES results acquired from sample 2 (process 2 in Table 1) are

Table 1
Experimental conditions

Process no.	Experiments	Ambient	Plasma source	Processing time (min)
Process 1 (sample 1)	Titanium ion implantation/deposition	Nitrogen gas	MEVVA	90
Process 2 (sample 2)	Titanium deposition, titanium and nitrogen ion implantation	Nitrogen plasma	MEVVA and filament glow discharge	90
Process 3 (sample 3)	(a) Titanium ion implantation/deposition	Nitrogen gas	MEVVA	10
	(b) Titanium deposition	Nitrogen gas	MEVVA	20
	(c) Nitrogen ion implantation	Nitrogen plasma	Filament glow discharge	20
	Repeat (b) and (c)			40

Table 2
PBII instrumental parameters

	Sample voltage (kV)	Frequency (Hz)	Pulse duration (μs)
Deposition	0	100	200
Deposition/implantation	0/20	100	170/30
Implantation	20	100	30

displayed in Fig. 3. Processes 2 and 3 yield a thicker film (2500 Å compared to 500 Å for process 1) corresponding to an effective deposition rate of ~ 0.5 Å s^{-1}. As the rise in the sample temperature is mainly due to the implanted ion flux [17,18], a low plasma density and implantation frequency were used in the low temperature processes described here. The substrate temperature is not directly monitored in these experiments, but based on previous work in which our in-situ thermocouple detector was in place, the substrate temperature here is lower than 150°C judging from the current waveform. However, it should be noted that a higher film deposition rate can be achieved through a higher plasma density and duty cycle if a higher temperature can be tolerated. Co-implantation of titanium and nitrogen ions in process 2 provides the target with more energy than either pure nitrogen ion implantation (process 3) or pure titanium ion implantation (process 1) alone and the sample temperature is highest in process 2. However, it should be noted that the temperature reached in process 2 is still quite low. In a separate experiment in which samples were treated using process 2 for different time, it was discovered that the interface thicknesses derived from Auger depth profiling data were comparable [19]. This illustrates that the sample temperature reached in this and the other two processes is low enough that thermal diffusion is not significant. A surface layer containing titanium, nitrogen and oxygen is observed on all three samples. Since our equipment does not operate in ultra-high vacuum (UHV) conditions, there is oxygen contamination in the residual vacuum. Even though oxygen is only a minor constituent in the plasma, the high oxygen content in the layer reflects the high adsorption rate of oxygen by a plasma-activated titanium or titanium nitride surface. It has been discovered that some residual species in the vacuum chamber may be beneficial to surface modification [20,21]. Our results are thus consistent and the effects of oxygen will be discussed later in this article.

The structures of the three samples were determined by glancing angle x-ray diffraction (GXRD) using the CuK_{α} excitation line. The lattice parameters are compared to the powder diffraction database. Fig. 4 exhibits the 2° grazing XRD spectra acquired from the three samples. The titanium and titanium nitrides (including TiN, Ti_2N) peaks are quite small due to the high intensity of the austenite phases of the SS304 base metal, but nonetheless, the formation of nitrides is evident. On account of the difference in the nitrogen incorporation mechanism, different titanium nitride contents are observed in the three samples. In process 2, nitrogen in the film comes from both direct implantation and absorption of nitrogen species from the overlying nitrogen plasma, and more TiN phases are observed. In comparison, less nitrogen is incorporated in process 1 (gas adsorption only) and process 3 (shorter exposure time to nitrogen plasma), and the TiN peaks are weaker than those in process 2.

The surface microhardness data obtained by a MATSUZAWA MXT-27 digital microhardness tester are shown in Fig. 5. All three treated samples show increased hardness which can be attributed to the formation of TiNO and the enhanced interfacial properties due to ion mixing. The microhardness of sample 3 improves by over 60% at a load of 25 g. Interestingly, although the film produced in process 1 is only one-fifth of that of sample 2 (process 2), their hardness results are nearly the same. Judging from the results, the depth

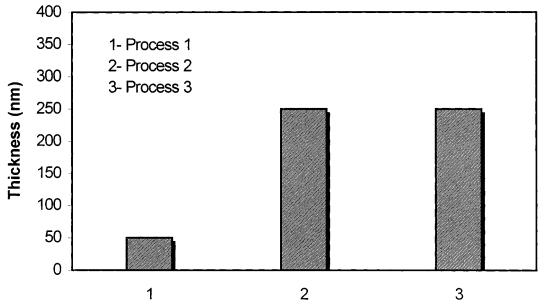

Fig. 2. Film thickness of the three samples determined by AES.

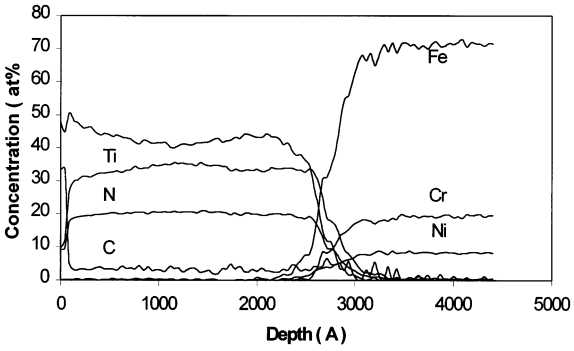

Fig. 3. Auger depth profile of sample 2 (process 2).

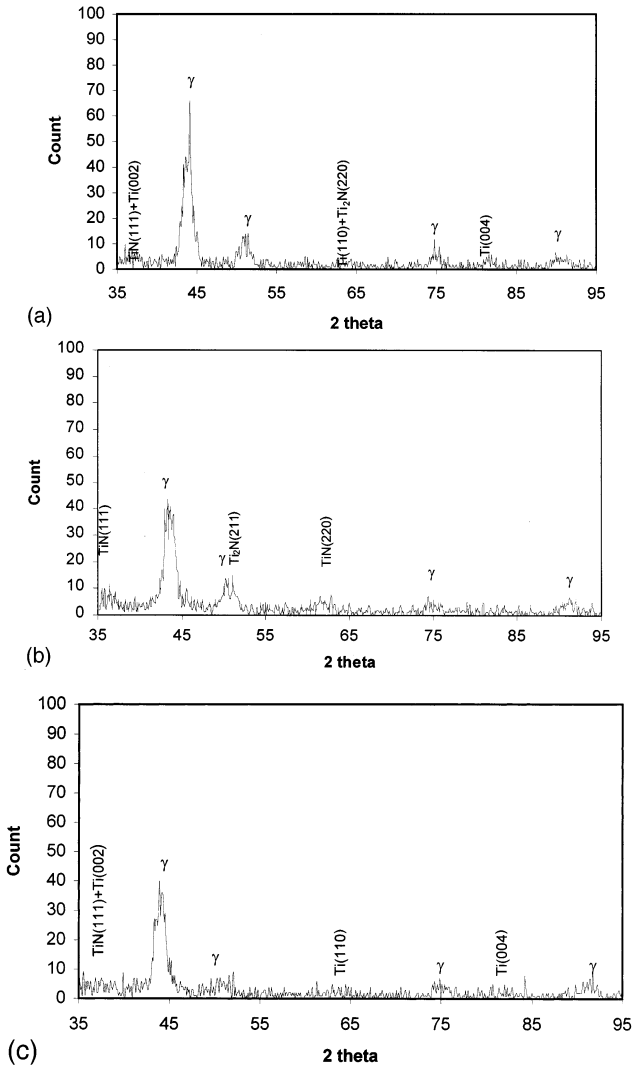

Fig. 4. Glancing X-ray diffraction spectra of: (a) sample 1 (process 1), (b) sample 2 (process 2), and (c) sample 3 (process 3).

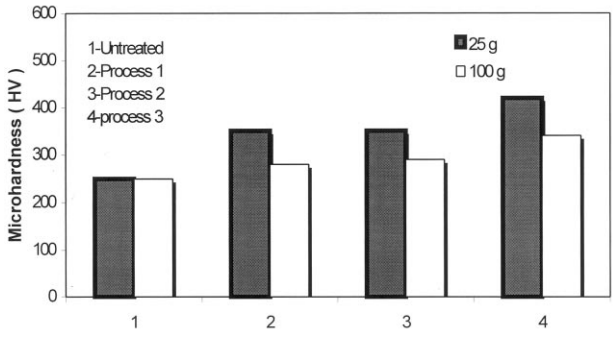

Fig. 5. Microhardness data at a loading of 25 and 100 g.

of the indent is larger than the TiNO film thickness which is less than 0.25 μm.

The tribological behavior of the untreated and treated samples is assessed using a pin-on-disk test. The wear tracks are investigated by Alpha-step stylus profilometry and scanning electron microscopy (SEM). In the pin-on-disk test, a 25 g load was applied to a 6 mm diameter silicon nitride ball without lubricants applied to the sample surface. The coefficients of friction as a function of the number of rotations are plotted in Fig. 6. The improvement is quite apparent for the treated samples. Sample 3 has a very low friction coefficient which remains at $0.15 \sim 0.20$ till the end of the test. Comparable frictional characteristics can also be observed for Ti6Al4V materials treated by PIII at above 500°C or plasma nitriding [22], confirming that our low temperature technique is as effective as conventional treatment at a much higher temperature.

The rate of wear can be determined by stylus profilometric measurements of the wear tracks, and the results are exhibited in Fig. 7. Each data point is an average of four measurements. After 500 turns, the cross-sectional area of the wear track on the untreated sample is as high as 25 μm^2. In contrast, the treated samples reveal smaller wear track size, with sample 3 showing the smallest wear and a wear track area of only 1.5 μm^2. The improvement is more than a factor of fifteen. The SEM micrographs displayed in Fig. 8 corroborate the wear track measurements by stylus profilometry. As shown in Fig. 8a, the untreated sample shows severe wear as well as adhesion, abrasion and plastic deformation in and around the wear track. The track is wide and deep, and consists of grooves up to $2000 \sim 3000$ Å in depth demonstrating severe metal sticking and tearing. The edges of the wear track are ragged and defor-

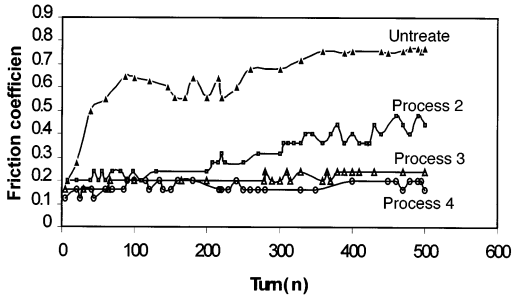

Fig. 6. Coefficients of friction versus number of turns determined by pin-on-disk test.

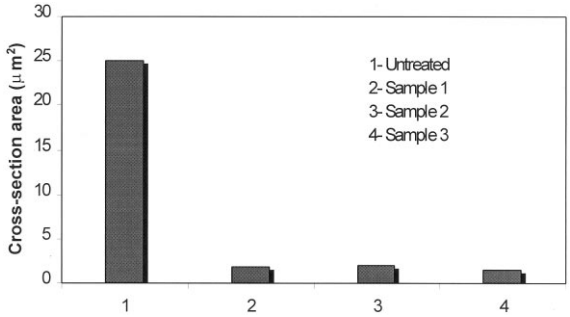

Fig. 7. Wear track cross-sectional areas obtained after 500 rotations at a loading of 25 g for the three samples.

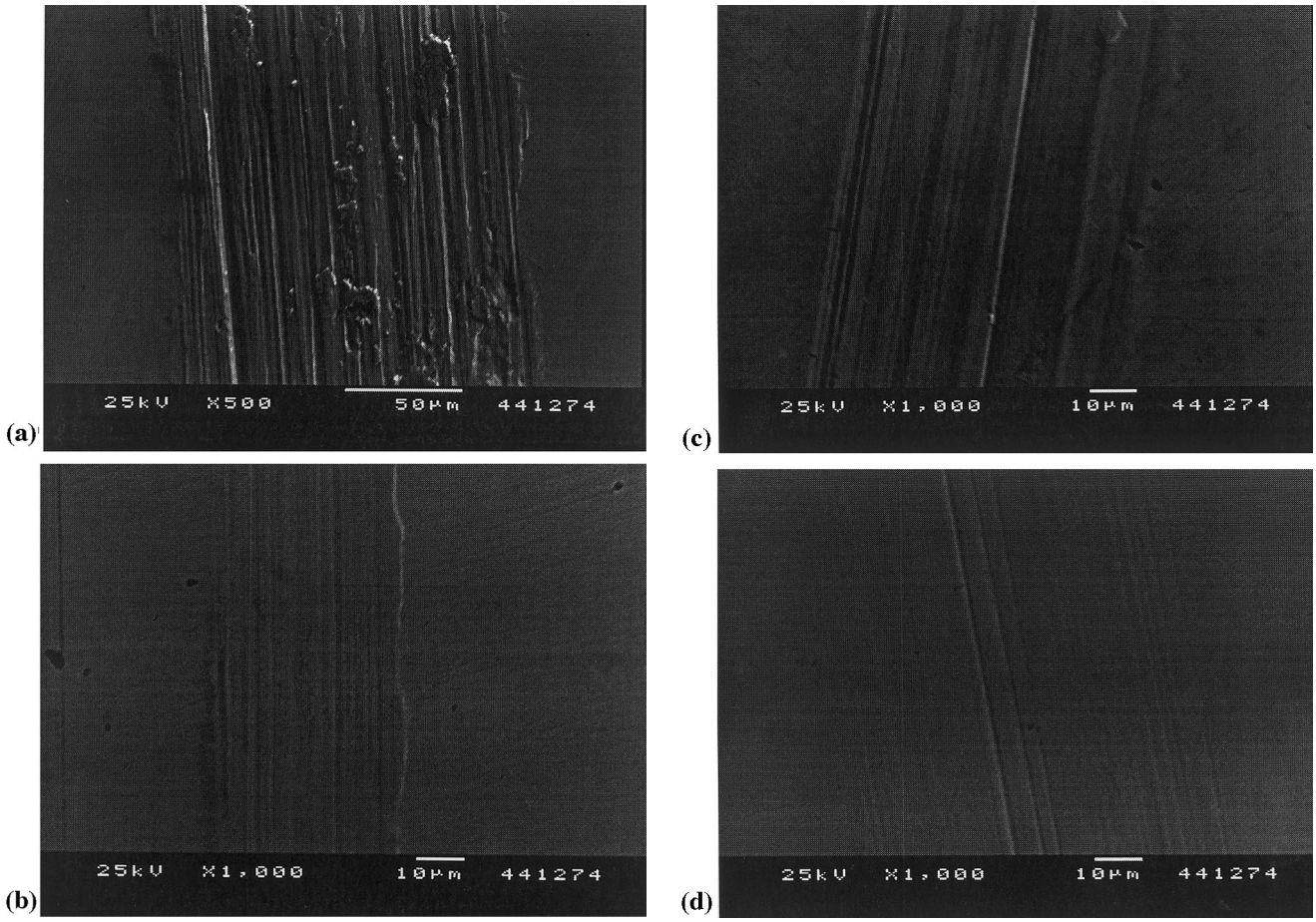

Fig. 8. Scanning electron micrographs of the wear tracks of: (a) untreated sample, (b) sample 1, (c) sample 2, and (d) sample 3.

mation slip bands have formed indicating plastic deformation of the materials close to the tracks. On the other hand, the wear track of the treated sample manifests as fine, shallow grooves without severe smearing. Based on the profilometric measurements, sample 3 shows the smallest and smoothest wear track. In comparison, slight plastic deformation and a deeper track are visible on samples 1 and 2. The tribological characteristics are consistent with the surface microhardness and friction coefficient data in that sample 3 possesses the lowest friction coefficient and the highest hardness among the three samples.

Our process is unique in that it combines metal and gas plasma treatment in a sequential or simultaneous way. The surface TiNO layer that enhances the surface properties is formed by deposition and ion implantation. The dynamic ion mixing process not only increases the strength of the film, but also the adhesion of the film to the substrate (inferred by the microhardness and pin-on-disk data). It is observed that if Ti is implanted/deposited in a nitrogen ambient (without nitrogen plasma formation), the film thickness is much smaller (process 1). We believe the reason to be excessive sputtering by the Ti ions without the mitigation effects of nitrogen. Anders et al. [23] have shown that only when the deposition to implantation ratio is small can excessive sputtering be circumvented and a thick film be formed. In processes 2 and 3, direct nitrogen ion implantation from the overlying plasma increases the amount of nitrogen available to form TiN and curbs the sputtering effects. The improvement on the microhardness and tribological properties can be ascribed to TiNO formation. In fact, the Ti to (N + O) ratio is nearly 2:3 confirming the co-existence and synergistic effects of TiN and TiO_2 [13,24] as TiO_2 provides additional hardening effects [25]. This may explain why process 3 produces the highest microhardness despite a relatively weak titanium nitride peak in the XRD spectrum. After all, it has been reported that nitrogen ion implantation into titanium alloys not only produces nitride in the near surface region, but promotes the formation of a smooth oxide film on the surface as well. At the same time, the oxide layer is stabilized by nitrogen [26–28]. We thus believe that the enhanced properties are the direct consequence of the synergistic effects of titanium, oxygen and nitrogen as well as dynamic ion mixing. The dominant mode of wear is changed to that of a mild, oxidative nature involving

the loss of fine oxide particles from the alloy surface. It thus follows that our dynamic PIII mixing process encompassing titanium deposition, titanium, oxygen, and nitrogen ion implantation, as well as oxygen adsorption yields superior tribological properties. Our observation is in line with that of direct oxygen ion implantation into Ti6Al4V [29–31]. In summary, our process increases the microhardness and stabilizes the treated surface by means of a protective layer consisting of titanium oxynitride which mitigates wear by retarding the detachment of abrasive oxide particles.

4. Conclusion

Titanium oxynitride layers are formed on 304 stainless steel by dynamic mixing plasma-based ion implantation. The thickness depends on the processing conditions. Pure Ti implantation/deposition yields the thinnest film due to unmitigated sputtering. When conducted together with nitrogen PBII, the film thickness increases by a factor of five. The sample treated by sequential Ti and N implantation/deposition has the best characteristics. This can be attributed to the synergistic effects of ion mixing and coexistence of titanium, oxygen, and nitrogen. The proposed process is very flexible, versatile, and suitable for complex-shaped samples. For example, by synchronizing the metal plasma and sample bias pulses, the process can be altered easily to perform 100% deposition, 100% implantation, or any deposition to implantation ratio. The significance of our results is that a low temperature plasma-based process can effectively produce a thick enough functional film with good properties and this should provide the needed impetus for the commercialization of plasma-based ion implantation.

Acknowledgements

The work was supported by Hong Kong Research Grants Council Earmarked Grants 9040332, 9040344, and 9040412 as well as the City University of Hong Kong Strategic Research Grant 7000964.

References

[1] J.R. Conrad, J.I. Radtke, R.A. Dodd, F.J. Worzala, N.C. Tran, J. Appl. Phys. 62 (1987) 4591.
[2] P.K. Chu, S. Qin, C. Chan, N.W. Cheung, L.A. Larson, Mater. Sci. Eng.: Reports R17 (6–7) (1996) 207.
[3] B.Y. Tang, P.K. Chu, S.Y. Wang, K.W. Chow, X.F. Wang, Surf. Coat. Technol. 103-104 (1998) 248.
[4] S.Y. Wang, P.K. Chu, B.Y. Tang, X.B. Tian, X.F. Wang, Q.Z. Lin, Thin Solid Films 311 (1997) 190.
[5] R. Wei, Surf. Coat. Technol. 83 (1996) 218.
[6] G.A. Collins, R. Hutchings, K.T. Short, J. Tendys, Surf. Coat. Technol. 103/104 (1998) 212.
[7] X.B. Tian, X.F. Wang, B.Y. Tang, P.K. Chu, P.K. Ko, Y.C. Cheng, Rev. Sci. Instrum. 70 (3) (1999) 1824.
[8] C. Blawert, B.L. Mordike, Nucl. Instrum. Methods B127/128 (1997) 873.
[9] J.R. Conrad, R.A. Dodd, F.J. Worzala, X. Qiu, Surf. Coat. Technol. 36 (1988) 927.
[10] J.N. Matossian, J. Vac. Sci. Technol. B12 (1994) 850.
[11] W. Ensinger, J. Hartmann, H. Bender, R.W. Thomae, A. Koniger, B. Stritzker, B. Rauschenbach, Surf. Coat. Technol. 85 (1996) 80.
[12] A. Koniger, W. Ensinger, C. Hammerl, T. Hochabauer, G. Schrag, J. Hartmann, R.W. Thomae, H. Bender, B. Stritzker, B. Rauschenbach, Nucl. Intrum. Methods B120 (1996) 282.
[13] Y. Chen, Y. Shi, H. Xie, Z. Wu, X. Jiang, T. Bell, H. Dong, Surf. Eng. 12 (2) (1996) 137.
[14] K. Volz, W. Ensinger, B. Stritzker, B. Rauschenbach, Surf. Coat. Technol. 103/104 (1998) 257.
[15] S. Schoser, J. Forget, K. Kohlhof, Surf. Coat. Technol. 93 (1997) 339.
[16] P.K. Chu, B.Y. Tang, Y.C. Cheng, P.K. Cheng, P.K. Ko, Rev. Sci. Instrum. 68 (4) (1997) 1866.
[17] G.A. Collins, R. Hutchings, K.T. Short, J. Tendys, C.H. Vandervalk, Surf. Coat. Technol. 84 (1996) 537.
[18] X.B. Tian, Z.N. Fan, X.C. Zeng, Z.M. Zeng, B.Y. Tang, P.K. Chu, Rev. Sci. Instrum. 70 (6) (1999) 2818.
[19] X.B. Tian, T. Zhang, Z.M. Zeng, B.Y. Tang, P.K. Chu, J. Vac. Sci. Technol. A17 (1999) 6.
[20] M.A. EI Khakani, H. Jaffrezic, G. Marest, N. Moncoffre, J. Tousset, Nucl. Instrum. Methods B50 (1990) 406.
[21] V.V. Vglov, V.V. Kammerl, B. Rauschenbach, Surf. Coat. Technol. 93 (1997) 331.
[22] S.M. Johns, T. Bell, M. Samandi, G.A. Collins, Surf. Coat. Technol. 85 (1996) 7.
[23] A. Anders, S. Anders, I.G. Brown, K.M. Yu, Nucl. Instrum. Methods B102 (1995) 132.
[24] H. Nagasaka, A. Chayahara, K. Fujii, Nucl. Instrum. Methods B121 (1997) 279.
[25] K. Fukushima, I. Yamada, Nucl. Instrum. Methods B112 (1996) 116.
[26] R. Hutchings, W.C. Oliver, Wear 92 (1983) 143.
[27] W.C. Oliver, R. Hutchings, J.B. Pethica, Metall. Trans. A15 (1984) 2221.
[28] S.R. Shephard, N.P. Suh, J. Lubr. Technol. 104 (1982) 29.
[29] F. Hohl, H. Berndt, P. Mayr, H.R. Stock, Surf. Coat. Technol. 74/75 (1995) 765.
[30] F. Alonso, A. Arizaga, J.J. Squainton, J. Ugaite, L. Uiviente, J.I. Onate, Surf. Coat. Technol. 74 (65) (1995) 986.
[31] A. Loinaz, M. Rinner, F. Alonso, J.I. Onate, W. Ensinger, Surf. Coat. Technol. 103/104 (1998) 262.